Design and Field Test of a Mass Efficient Crane for Lunar Payload Handling and Inspection: the Lunar Surface Manipulation System

William R. Doggett[1]
NASA Langley Research Center, Hampton VA, 23681

Bruce D. King[2]
Lockheed Martin Mission Services, Hampton VA, 23681

Thomas Carno Jones and John T. Dorsey[3]
NASA Langley Research Center, Hampton VA, 23681

and

Martin M. Mikulas[4]
National Institute of Aerospace, Hampton VA, 23681

Devices for lifting, translating and precisely placing payloads are critical for efficient Earth-based construction operations. Both recent and past studies have demonstrated that devices with similar functionality will be needed to support lunar outpost operations. Lunar payloads include: a) prepackaged hardware and supplies which must be unloaded from landers and then accurately located at their operational site, b) sensor packages used for periodic inspection of landers, habitat surfaces, etc., and c) local materials such as regolith which require grading, excavation and placement. Although several designs have been developed for Earth based applications, these devices lack unique design characteristics necessary for transport to and use on the harsh lunar surface. These design characteristics include: a) composite components, b) compact packaging for launch, c) simple in-field reconfiguration and repair, and d) support for tele-operated or automated operations. Also, in contrast to Earth-based construction, where special purpose devices dominate a construction site, a lunar outpost will require versatile devices which provide operational benefit from initial construction through sustained operations.

This paper will detail the design of a unique, high performance, versatile lifting device designed for operations on the lunar surface. The device is called the Lunar Surface Manipulation System to highlight the versatile nature of the device which supports conventional cable suspended crane operations as well as operations usually associated with a manipulator such as precise positioning where the payload is rigidly grappled by a tool attached to the tip of the device. A first generation test-bed to verify design methods and operational procedures is under development at the NASA Langley Research Center and recently completed field tests at Moses Lake Washington. The design relied on non-linear finite element analysis which is shown to correlate favorably with laboratory experiments. A key design objective, reviewed in this paper, is the device's simplicity, resulting from a focus on the minimum set of functions necessary to perform payload offload. Further development of the device has the potential for significant mass savings, with a high performance device incorporating composite elements estimated to have a mass less than 3% of the mass of the maximum lunar payload lifted at the tip. The paper will conclude with future plans for expanding the operational versatility of the device.

[1] Senior Research Engineer, Structural Concepts and Mechanics Branch, MS-190, Member.
[2] Senior Designer
[3] Senior Research Engineers, Structural Concepts and Mechanics Branch, MS-190, Associate Fellows
[4] Senior Research Fellow, Fellow, AIAA.

Nomenclature and Abbreviations

c1	=	compression member forming crane king post
c2	=	compression member forming crane arm
c3	=	compression member forming crane forearm
FEM	=	finite element model
Hab	=	habitat
ISRU	=	In Situ Resource Utilization
LSMS	=	Lunar Surface Manipulation System
s1	=	spreader located near waist separating hoist2 line of action from kingpost
s2a	=	first spreader counterclockwise from arm at top of king post used to separate hoist3 line of action from arm
s2b	=	second spreader counterclockwise from arm at top of king post used to separate hoist2 line of action from kingpost
s3a	=	first spreader counterclockwise from forearm at elbow used to separate hoist3 line of action from forearm
s3b	=	second spreader counterclockwise from forearm at elbow used to separate hoist3 line of action from forearm
t3a	=	tension member forming arm diagonal support rod
t2b	=	tension member connecting s2a to s2b
t2c	=	tension member connecting s2b to cable 2
TER	=	three element rosette strain gauge
UA	=	uniaxial strain gauge
θ_1	=	crane waist rotation
θ_2	=	crane shoulder rotation
θ_3	=	crane elbow rotation

I. Introduction and Lunar Surface Manipulation System Overview

Devices for lifting, translating and precisely placing payloads are critical for efficient Earth-based construction operations. Both recent and past studies have demonstrated that devices with similar functionality will be needed to support lunar outpost operations.[1,2] Lunar payloads include: a) prepackaged hardware and supplies which must be unloaded from landers and then accurately located at their operational site, b) sensor packages used for periodic inspection of landers, habitat surfaces, etc., and c) local materials such as regolith which require excavation and grading.[3] Although several designs have been developed for Earth based applications, these devices lack unique design characteristics necessary for transport to and use on the harsh lunar surface.[4] These design characteristics include: a) lightweight components, b) compact packaging for launch, c) automated deployment, d) simple in-field reconfiguration and repair, and e) support for tele-operated or automated operations. Also, because the cost to transport mass to the lunar surface is very high, the number of devices that can be dedicated to surface operations will be limited. Thus, in contrast to Earth-based construction, where many single-purpose devices dominate a construction site, a lunar outpost will require a limited number of versatile devices which provide operational benefit from initial construction through sustained operations.

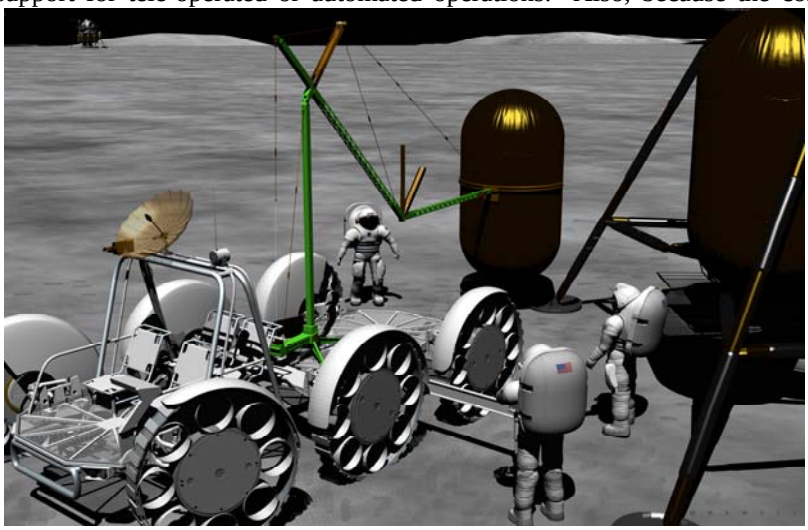

Figure 1. Rigid Grapple of Tank to Support Reuse of Lander Components.

This paper will detail the design and testing of a unique, versatile lifting device designed for operations on the lunar surface. Testing has included

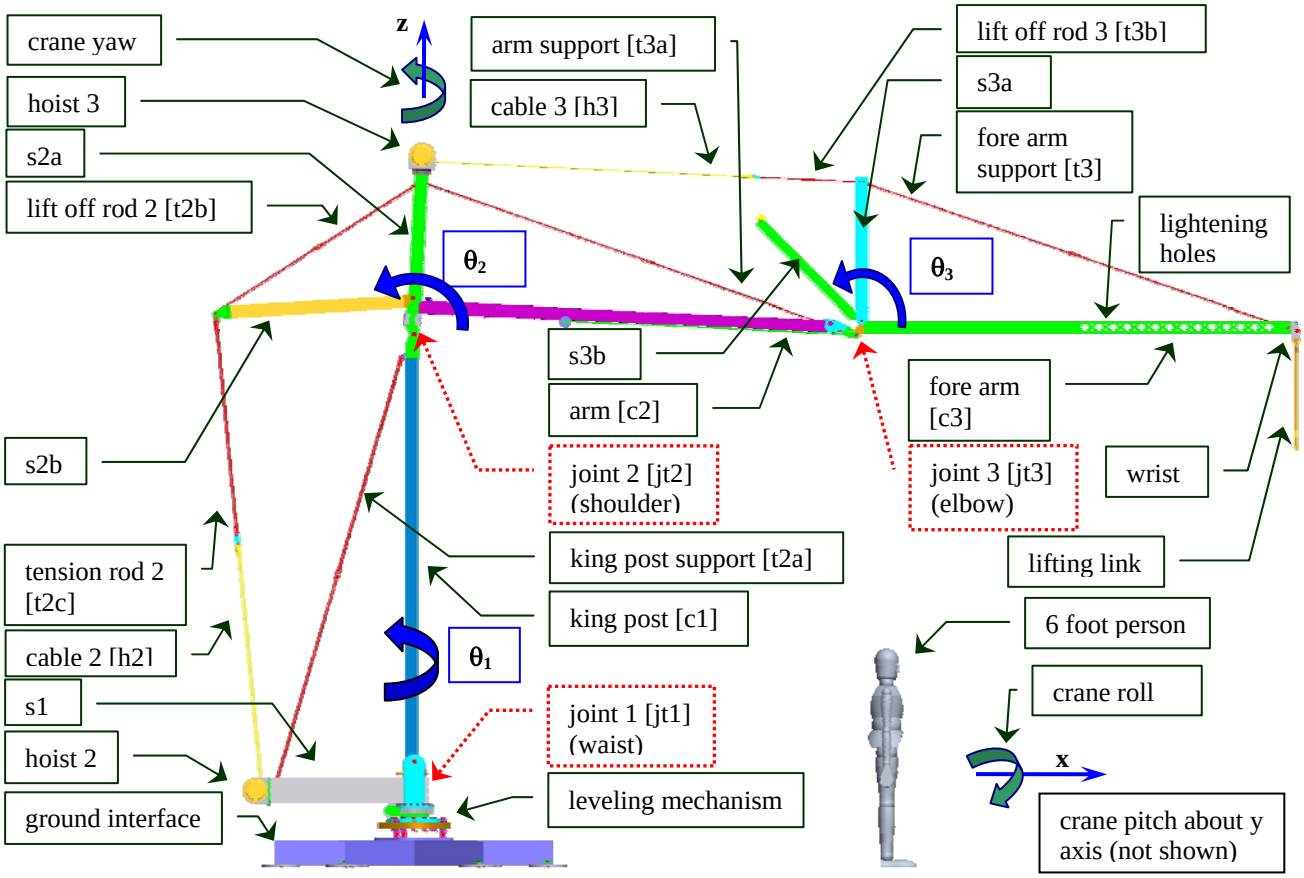

Figure 2. LSMS Naming Convention.

laboratory load tests which were correlated with finite element analysis as well as field tests near Moses Lake, Wa to verify the operational performance of the first generation device in an unstructured environment interacting with mobility devices.

The device is called the Lunar Surface Manipulation System (LSMS) to highlight the versatile nature of the device which supports both conventional cable suspended crane operations as well as precise positioning where the payload is rigidly grappled by a tool attached to the tip of the device. The operational versatility of the LSMS arises from a modular design that supports planetary surface reconfiguration and the use of interchangeable tools. These tools allow the device to adapt to planned as well as future needs. An example of this versatility is shown in Fig. 1, where a tank is removed from underneath a lander by the LSMS mounted to a rover using a side grip/grapple. The advanced structural architecture of the device results in a lightweight design. A high performance variant incorporating composite elements is estimated to have a mass of less than 3% of the mass of the maximum lunar payload lifted at the tip or 1.8 % of the lunar mass lifted at the boom's mid-span.[5] A great deal of design effort was directed at careful management of the structural loads and the use of simple tension and compression members to facilitate integration of composite members. The test-bed device demonstrates the ability of the device to package compactly for launch. Automated deployment has not been incorporated into this first generation device.

II. Lunar Surface Manipulation System First Generation Test-Bed Design

To verify and refine procedures and hardware to support off-loading and precision positioning of payloads for planetary surfaces, a first generation test-bed of the LSMS was constructed at NASA Langley Research Center. A governing tenet during the design was to only include capabilities necessary to perform the intended offloading function. This resulted in a robust device with minimal complexity. Fig. 2 shows a CAD model of the test-bed with major elements named. The device's structural efficiency derives from the truss design of the boom and the mechanical advantage provided to the actuators. Like a crane, the actuators (hoist 2 and 3) are not located at the joints, but are offset from the joints and act on lever arms called spreaders which rotate about the joints providing mechanical advantage and thus reducing motor performance requirements.[6] The spreaders are identified in Fig. 2 by

a leading "s" followed by a number indicating the joint about which they provide mechanical advantage and then a letter that is assigned consecutively to each spreader in a counter clockwise direction from the horizontal. For example, "s2a", is the spreader that provides mechanical advantage about the second joint (i.e. the shoulder) with "a" indicating it is the first spreader encountered in a counterclockwise direction from the horizontal.

The diagonals of the truss are formed from fixed length tension rods, labeled arm support, forearm support and kingpost support respectively. Lift off rods are present to connect spreaders, s2a and s2b as well as s3a and s3b. These lift off rods provide a unique capability that will be detailed later in the paper.

The LSMS has a tall narrow structural architecture with an inner compression structure formed by the kingpost, arm and forearm and an outer tension structure formed by the cables connected to hoists, tension rods and support rods. The test-bed has 3 degrees of freedom, labeled in dashed call outs in Fig. 2. Beginning at the base there is a waist rotation, θ_1, about the z axis followed by shoulder rotation, θ_2, at the top of the king post about an axis out of the page of the figure followed by an elbow rotation, θ_3, at the intersection of the arm and forearm about an axis out of the page. Also shown in the figure are the leveling mechanism and ground interface that will be detailed below.

A. Design Constraints for Test-Bed

Before describing the test-bed design in detail it is important to understand that schedule and funding limitations imposed constraints on the design. These constraints resulted in the use of off the shelf motors, hoists, drive electronics, and structural extrusions. A great deal of design effort was expended to maintain the important characteristics of the LSMS within these constraints. For example, the structural architecture of the LSMS was specifically designed to take advantage of composite members as will be described in the next section, however constructing a composite device was deemed too expensive for the first generation test-bed. Additionally, the members near the tip are subjected to significantly less load than those near the base; however their dimensions were fixed by the design of the highest loaded member. In the case of the compression members, the kingpost design set the size for all of the square cross sectioned members which included s2b, arm, and forearm. An effort was made to reduce the weight in the forearm, as is evident by the lightening holes at the wrist end of the forearm (Fig. 2). Similar weight reduction is possible in most of the other structural elements.

B. Design Details

The LSMS is sized to: lift a metric ton at the tip on the lunar surface, to have a reach of 7.5 m (24.6 ft) and to stand 3.8 m (12.5 ft) at the shoulder to be capable of off loading landers with a 5 to 6m (16.4 to 19.7 ft) deck height. The basic objective of the design was to minimize complexity and maximize simplicity. By that, it is meant to use the minimal functions that accomplish the task objectives (i.e. minimize the number of degrees of freedom, size, joint range and control complexity of the device). Simple shapes, standard extrusions, two-dimensional parts and commercial off the shelf components were used before other alternatives were considered.

To be a viable design, secondary requirements were also imposed on the design including robustness to dust contamination from the lunar regolith, minimizing the number of rotating parts, deployment from the stowed flight configuration, and protection for the wiring. For the dust contamination it was thought that bellows could provide protection as they could be sized to fit around components as needed, potentially enclosing the entire line of action for the hoist cable combination. For example, a bellows could be used to enclose the entire hoist 2 system and cable up to the attachment interface between "tension rod 2" and "cable 2" of Fig 2. To minimize the number of rotating parts, or more accurately, the number of pinned joints, connection points for components were consolidated. Several deployment scenarios have been discussed for erecting the system, with the most promising being a lighter cable wound onto each cable drum that would retract ahead of the main cable during deployment and remain permanently on the drum since deployment is considered a one-shot event. Hoist cabling has been simplified to include no pulleys or guides that would alter the cable path and cause cable abrasion. Each cable feeds out directly from the drum. In the future, cables may be replaced by thin flat metallic strips that would lay on the drums like a strap to reduce torsion on the hoist mounts resulting from the change in cable angle as cable tracks across the drum. To simplify the wiring, all of the wires route internally through the system structure. This greatly reduces the risk of damage from

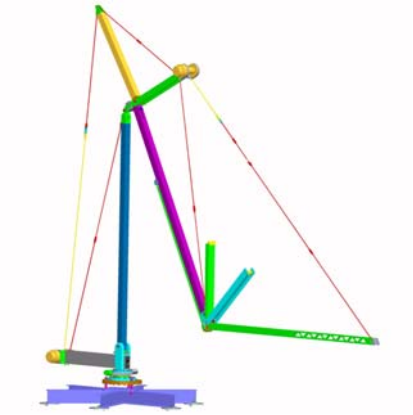

Figure 3. Tension Members Lifted Off s3a and s3b with LSMS in Fork-Lift

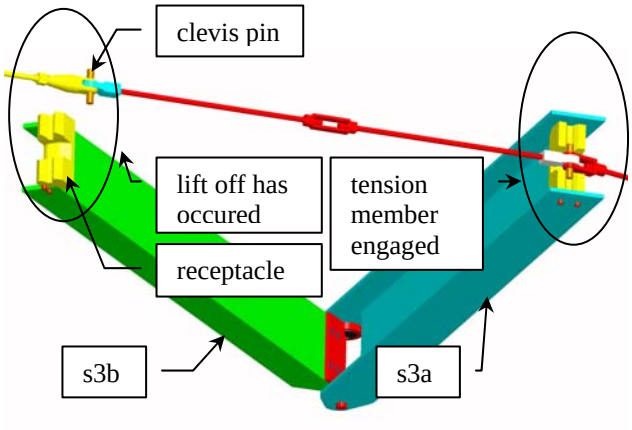

Figure 4. Hardware Detail Supporting Tension Member Lift Off.

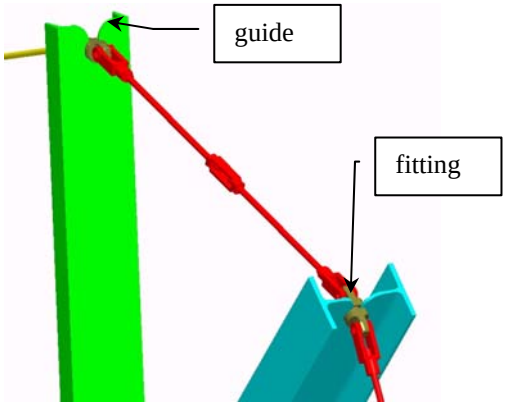

Figure 5. Early Concept Supporting Tension Member Lift Off

chafing or external contact. Details of unique features of the design will be described next beginning with the spreaders.

1. Spreader Cable Interface Supporting Tension Cable Lift off

The spreaders; s1, s2a, s2b, s3a and s3b of Fig. 2, are used to provide mechanical advantage to the motors about the joints and provide separation between the tension and compression members in the structural architecture. The spreaders behave like spokes on a wheel as the arm and forearm rotate over a large articulation range enabling the LSMS to place reach below its base to provide payload handling capabilities from Landers or into trenches.

Tension member lift off enables a large articulation range for both the arm and forearm enabling configurations such as the fork-lift configuration shown in Fig. 3. Fork lift configuration provides access to payloads under a lander deck, within a vehicle or beneath a shelter. A scheme was needed to allow the cable to disengage and engage smoothly from the top of the spreader as illustrated in Fig. 4. This is accomplished by slightly increasing the clevis pin length to enable it to nest into a receptacle at the end of the spreaders. Figure 4 details the associated hardware, with the connection at the top of s3a engaged on the right of the figure and the connection at the top of s3b lifted off on the left.

The design shown in Fig. 4 is the final as built concept. The design reduces the number of components and eliminates offsets at the connections and joints simplifying the analysis. Note that the pin is aligned along the neutral axis of the spreaders. For contrast, an earlier design is shown in Fig. 5 where a machined fitting engaged guides at the top of the spreaders. This design introduced undesirable offsets between adjacent connections as well as offsets to the neutral axis of the spreader as well as additional mass compared to the design of Fig. 4. In addition, there is a slight change in engagement angle as the fitting slides down the guide which introduces a tendency to jam. These problems were eliminated with the final concept of Fig. 4.

2. Spreader Nesting for Compact Packaging

Spreader nesting, for stowage, was an initial design consideration for both the s3a and s3b spreaders. After a multitude of shapes, cross-sections, pivot locations and nesting configurations were examined, the design shown in Fig. 6, utilizing an offset pivot for nesting the s3a and s3b spreaders in the stowed position proved to be the most efficient solution. In Fig. 6 the image on the left displays the spreaders deployed, while the image on the right shows the spreaders nested in their stowed positions. A single hardware pin is used for the actual mounting. s3b rotates about an axis raised above s2a via the s3b attachment fitting shown in Fig. 6. s2a rotates about the spreader pin directly.

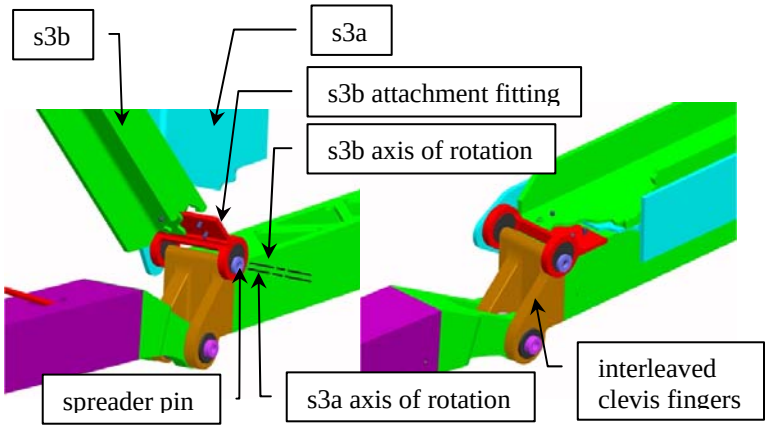

Figure 6. Elbow Joint Detail and Spreader Nesting for Packaging

The spreaders at the top of the kingpost, s2a and s2b, utilize a similar pinning arrangement to accomplish the nesting for stowage.

3. Offset Clevis for Increased Joint Stiffness

The joint is formed using a pair of interleaved clevis fingers as shown in Fig. 6. This arrangement keeps the spread between the clevis fingers the same on both sides of the joint significantly increasing the stiffness over a more common symmetric design.

4. Lifting Links Provide Stiff Connection to Payload

Lifting links, identified in Fig. 7, were designed as a structurally stiff means of connecting the LSMS to a payload. In contrast to cables and slings which have a tendency to stretch as load is applied and supply little torsional stiffness, the lifting links act more like a rigid member. Each Link is essentially a thin I-beam with pinned ends. A hook (shown in the detail on the right of Fig. 7) applicable to any of the payloads was designed to slip easily onto the pinned end of a lifting link. The sloped face on top of the hook guides the pin as the lifting link is lowered into position over a payload. In addition centering guides, one of which is identified in Fig. 7, are affixed to the lifting link pin to provide precise alignment and centering as the hook is engaged. The capture envelope is on the order of +/- 10 degrees about roll and yaw axes of the crane (identified in Fig. 2) and +/- 90 degrees about the pitch axis of the crane base.

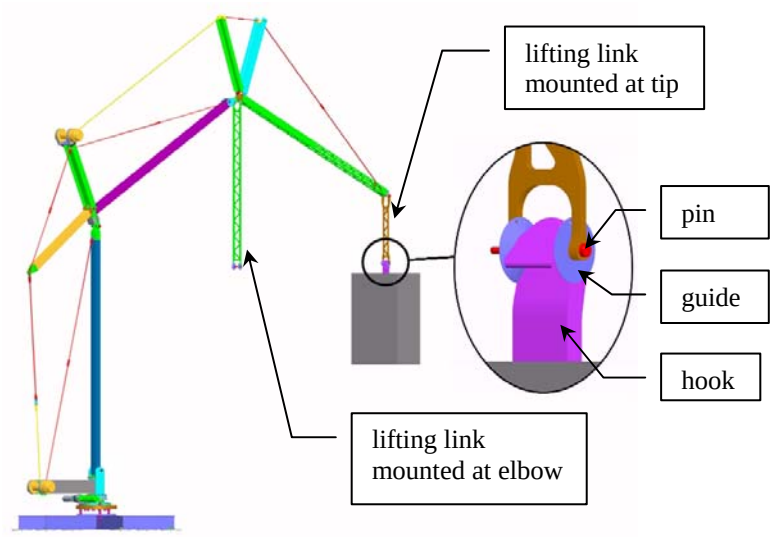

Figure 7. Lifting Links Provide Structurally Stiff Connection to Payload

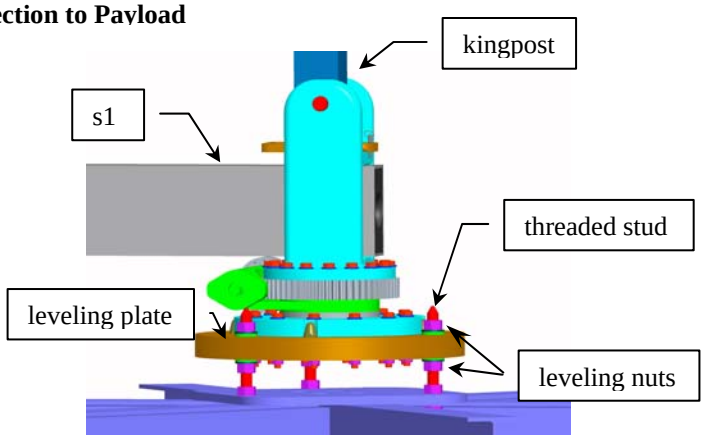

Figure 8. 3 Post Leveling System for LSMS

5. Three Post Base Provided Straight Forward Leveling

A three post leveling system was designed and incorporated into the LSMS support base, Fig. 8. The first generation design supported rapid transition of the crane from an elevated platform to the ground mount. The design supported leveling over a +/- 5 degree angle range by manually rotating a pair of opposing leveling nuts that captured a leveling plate along a threaded stud. Note the top of the threaded studs are cone shaped providing an alignment aid. Critical to successful transitions between the elevated platform and ground mount was the ability to rotate the base flange as the LSMS was lowered on the studs. Automating the design is straightforward by replacing the pair of rotating nuts with a captive nut driven by a motor. Automating the design is a critical capability for an automatic leveling and automatic repositioning of the waist. The LSMS architecture supports fixing the wrist, and then lifting and repositioning the waist, effectively allowing the LSMS to walk off or onto an elevated lander or move from a mobile base to a ground base under its own power.

6. Vee-groove Mechanical Interface for Tools

A Vee-groove dovetail arrangement is used at the end of the forearm to provide a quick-connect to attach tools as shown in Fig. 9. This design allows rapid automated

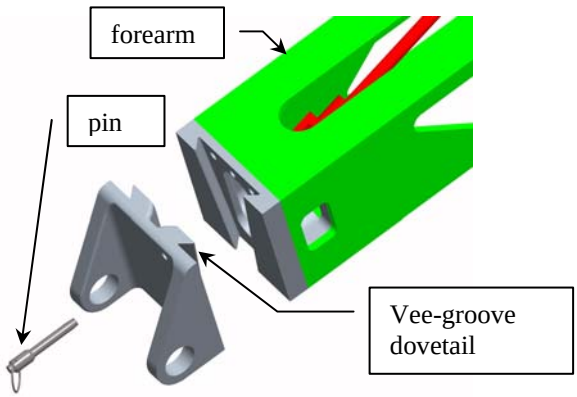

Figure 9. Mechanical Interface for Tools at Wrist

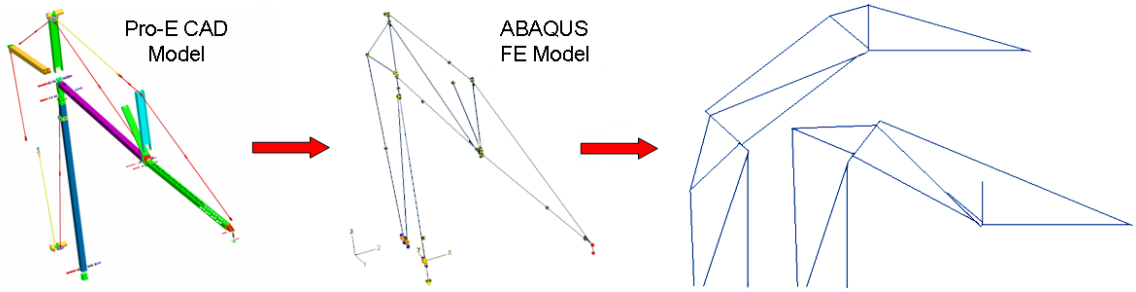

Figure 10. FEM model of LSMS with Different Arm/Forearm Angles Specified

exchange of tools such as the lifting links shown in Fig. 7. Currently, after the two halves of the fitting have slid together, a pin (shown in Fig. 9) is inserted to lock them in place. The pin is planned to be replaced by a plunger in the future to support fully autonomous exchange. This design was selected because it has a large capture envelope, is dust tolerant and tends to firm up as a load is applied.

C. Design Verification

To predict the geometric shape and internal stresses of the LSMS, a detailed finite element model (FEM) was constructed using the ABAQUS FEM package. Due to the high length to diameter of the structural members, the model uses highly efficient shear flexible beam elements (B31). A minimum of 10 nodes are used per member with a fixed nodal density throughout the model. The finite element assembly includes all offsets at the joint locations, and models the pinned joints explicitly as kinematic coupling constraints with one degree of freedom in rotation (Fig . 10). To allow the user to analyze the LSMS for any given arm or forearm angles, while allowing for cable lift-off and re-engagement, a script was written using the ABAQUS Application Programming Interface (API). The ABAQUS API allows programs to be created that can interface directly to the models and data used by ABAQUS. The LSMS script only requires the location of key nodal positions and the angles of the arm and forearm. Using this data it creates a new model, determines the correct cable state (engaged or lifted-off the spreaders), applies the mesh, defines the joints and sets up the boundary conditions and load state. Finally it runs static and buckling analyses and can write the stresses, strains, loads and displacements to a text file. The analyses use the nonlinear geometry option (NLGEOM) to account for the geometric stiffness of the cables under gravitational and applied loads. The script allows rapid exploration and analysis of parameters in the model and design changes can also be easily and efficiently incorporated.

To verify that the finite element model could predict the structural behavior of the LSMS, load tests were performed on the first generation LSMS, constructed in the James H Starnes, Jr. Structures Laboratory at Langley Research Center. A combination of 19 Uniaxial (UA) and 13 Three-Element Rosette (TER) strain gauges were applied to key members of the structure and a single 5000 N load cell was attached inline with the t2c tension rod (Fig. 11). The strain gauges are accurate to 0.3±0.2% and measured either pure axial strain (UA) or strain in all three principal directions (TER). The strain and load data was collected using a Vishay System 5000, model 5100A data acquisition system running Strainsmart software. Test data was taken at 1 Hz. The TER strain gauges were applied to the primary horizontal members as shown in Fig. 11**,** at positions 1,2,3 and 4. 6 UA gauges were applied around the front portion of the forearm (position 5) where lightning holes had been cut. The remaining UA gauges were attached to the vertical spreaders and to the t2b and t3a diagonals (positions 6~9). A load cell was located inline with the t2c tension rod as a control, to have a direct load reading during the test (position 10).

The load tests were performed by successively adding 10, 20 or 50 lb plates to a 10lb weight rack attached to the tip of the LSMS. This method was chosen for its simplicity and it allowed a visual confirmation of the load level during the tests. The strain gauges and load cell were tared with zero load at the tip. The weight rack was then attached and the plates individually weighed and added, up to a peak load of 390 lbs, or 118% of the 330 lb design tip load. Between each quasi-static addition of a plate, the LSMS was allowed to settle from any induced vibration. Once the strain and load measurements stabilized, the next plate was added. Measurement data was taken continuously from the initial tare up to the peak load level.

The data from the LSMS load test was reduced and compared with the results of the finite element model using the procedure outlined in Fig. 12. The strain and load measurements from the test were recorded in an excel spreadsheet and transferred to a text file. A Matlab program was written to read in the data and combine the strain readings from each sensor to form a data set for all 32 strain measurements and the load cell. As the data was recorded continuously, the strain and load measurements versus time had to be partitioned to extract the data for each tip load. This was done by averaging the steady state strain or load level after it was allowed to stabilize. Static load finite

element analyses had been performed prior to the test for the desired load cases and the axial strains at the strain gauge locations and load in the t2c tension rod were saved to a data file. This file was read into the Matlab program for processing and comparison to the test data. Each set of strain or load vs. tip load data had a linear regression performed on it and the results from the test and the FE analysis were compared. For the purposes of the comparison, only the axial data from the sensors was used and the average was taken at each position. Gravity was included as a nonlinear effect in the model to account for the sag in the cables and the additional geometric stiffness they provide that would not be included in a linear analysis. The strain and load results for the static analysis were then zeroed for the base case, under gravity but with zero tip load, as in the test article.

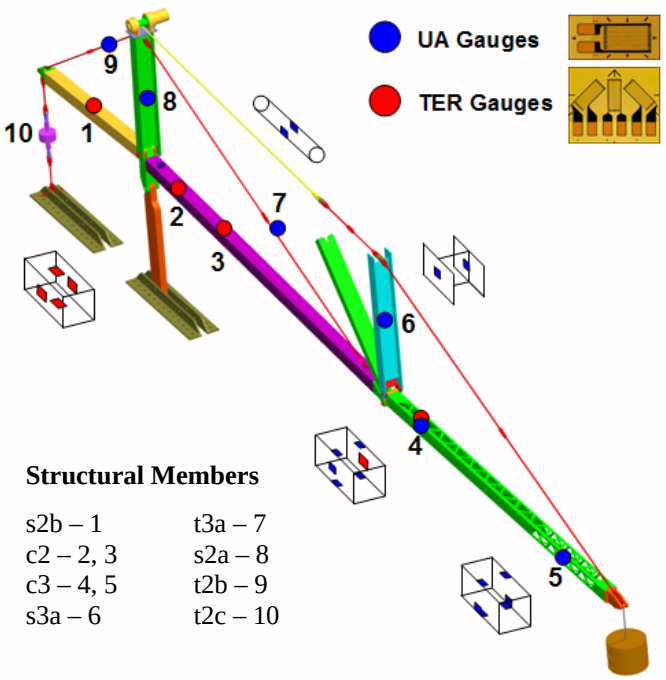

Figure 11. Strain Gauge and Load Cell Locations

The results of the test measurements, and comparisons to the FEM results are plotted in Fig. 13. It can be seen that the FE model very closely correlates with the test data plotted as symbols. The error for all members, but the front portion of the forearm (position 5) was less than 5% over the range of applied tip loads. The following members had errors of <2%: s2b, t3a, t2b and c3 (Position 4). The compression elements, including the spreaders and the arm tended to have slightly higher error than the simple tension elements. The large discrepancy between the test and FEM for the outer portion of the forearm merits some discussion. The forearm has lightening cut-outs in the top and bottom along the entire length. In addition, from approximately the mid-span to the tip there are additional cut-outs along the sides. (Fig. 2). These create a truss pattern that reduces the weight of the member while maintaining a stiff structure. More material was removed from the top and bottom because the elbow spreader acts to cut the critical Euler column buckling length in half of the arm/forearm combination for buckling perpendicular to the (x,y) plane of Fig. 2 compared to buckling perpendicular to the (x,z) plane. The bending moment of inertia, calculated as an input to the FE model, used a conservative approach by considering there to be no cross bracing where the cut-outs occurred. This reduces the stiffness of the forearm, thus predicting higher strains in the model then measured in tests. The use of beam elements requires the calculation and simplification of complex cross-sections such as the trussed beam or even the I-beam spreaders. This can be a source of error and must be correlated to experimental results, as were conducted in this study. The individual strain measurements of the six UA gauges at position 5, also showed some incongruity. For a purely in-plane load test, like the one conducted, one would expect to see equal strains in the top two sensors, and similar equality in the bottom two. This however is not the case, and the results suggest that the forearm was bending out-of-plane. Strangely however, the top and bottom sensors show opposite bending directions. It is possible the strain gauges were misaligned, although on inspection this didn't appear to be

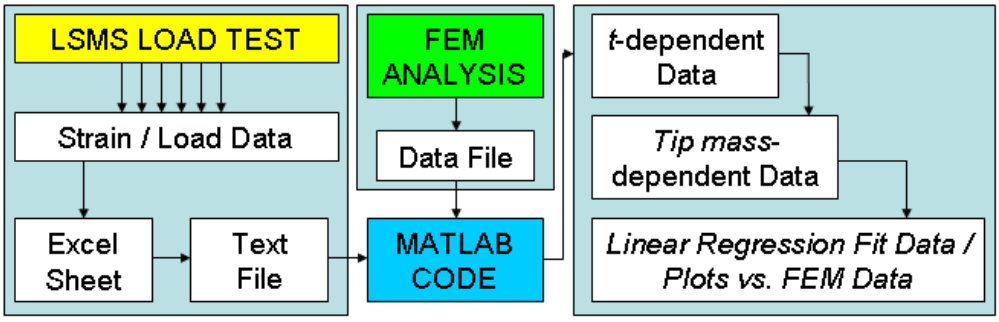

Figure 12. Outline of Data Reduction and Comparison from LSMS Load Test

the case.

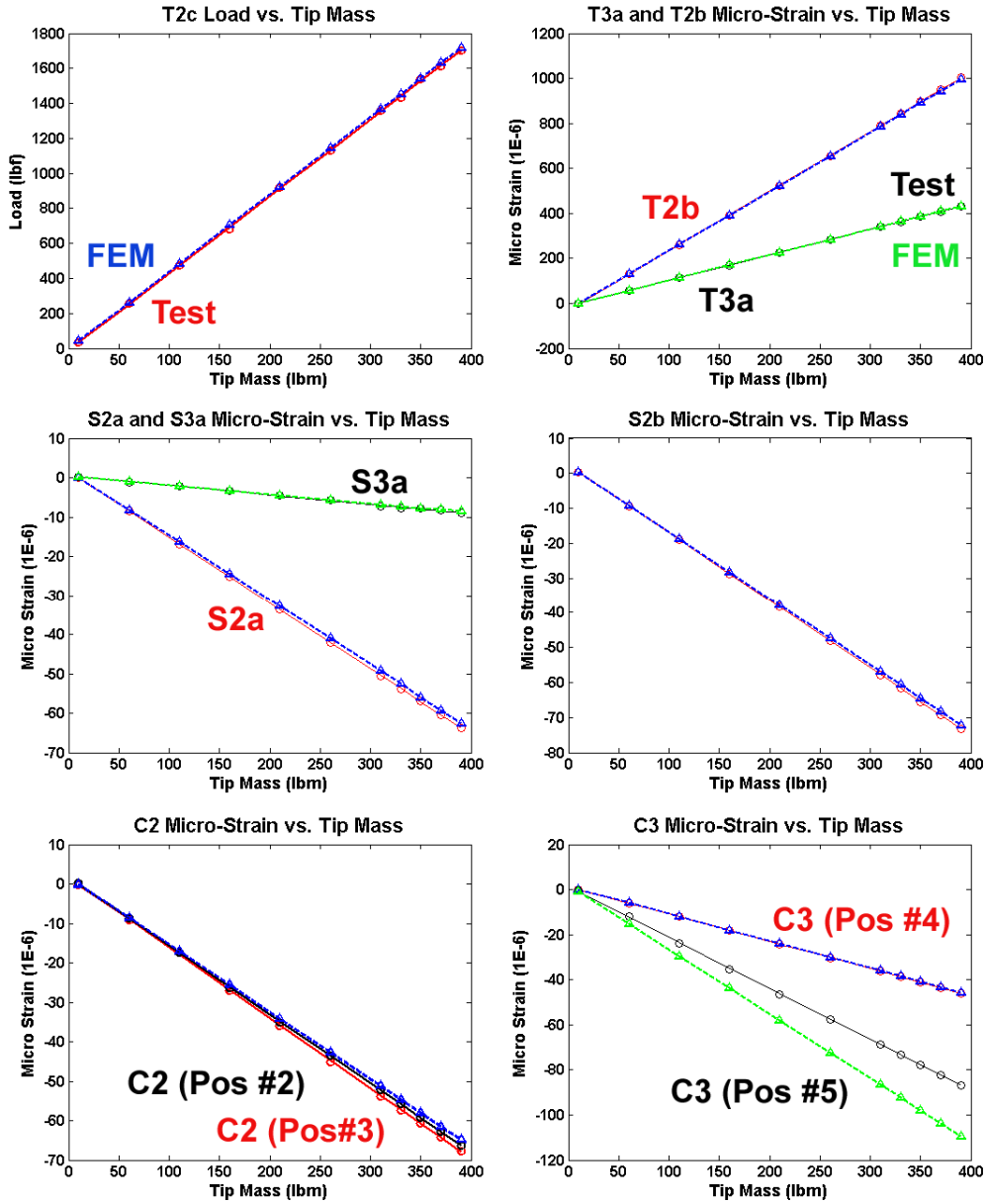

Figure 13. LSMS Load Test Comparison to FE Model Results

Although the FE model proved to be remarkably accurate, there are several additional factors that could lead to differences in the analytical and experimental results. At very low strains, the sensitivity of the gauges is reduced. This coupled with non-linearities in the joints can cause disparity between the model and test results at low loads. The test was run in a working lab using a very simple loading device (the weight rack), and low level vibrations from human interaction and background machinery remained in the data. The average reading of the oscillatory data for all inputs was then based at least partially on user judgment. Lastly, the modulus of elasticity and 'stretched' cross-sectional area of the cable members was not tested a priori, and could have impacted the strains that were measured. Linear behavior of the cables was also assumed.

A tensile test was also performed on the rod stock used for the tension diagonals to find their ultimate load. The rods used for the LSMS are fully-threaded, 3/8-24", B7 steel and have a rated ultimate strength of 125 Ksi and a yield strength of 105 Ksi. The tested rods failed cleanly at 11,846 Ibf (116 Ksi) or 93% of the rated strength. At the maximum design tip mass of 330 Ibs, the highest load in any of the tension members (in t2b) is 3867 Ibf. Thus in the worst case we are operating at 33% ultimate load for the rods and are well within the elastic region.

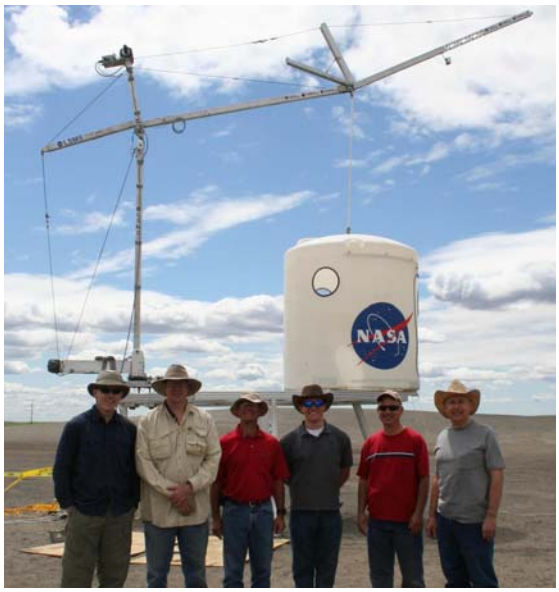

Figure 14. LSMS Team (L to R): Tom Jones, Bill Doggett, Dorsey, Mike Grimes, Dave Mercer, Bruce King

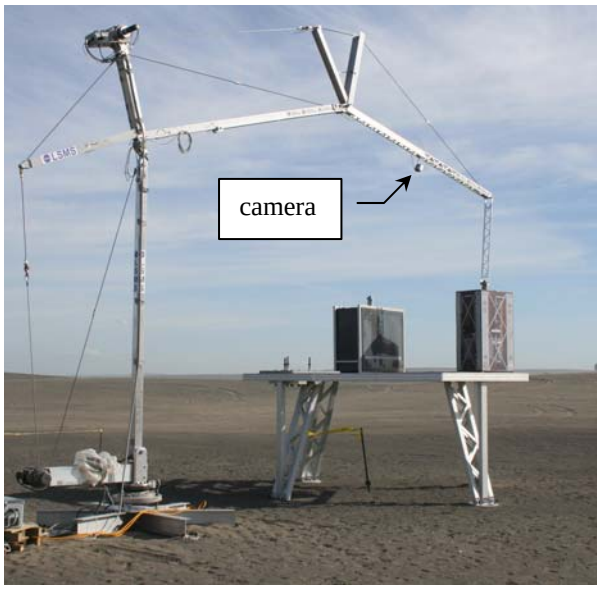

Figure 15. LSMS on Ground Mount Offloading Simulated ISRU Package from Elevated Platform.

III. Moses Lake Field Test Results in Conjunction with Human Robotics Systems Project Team

The LSMS team, shown in Fig. 14, was active in field tests at Moses Lake WA from May 31st to June 13th 2008. The objective of the tests were to evaluate the performance of the LSMS in an unstructured environment as well as to investigate the LSMS operations in conjunction with mobility assets. These mobility assets are under development by other team members. ATHLETE is under development by Jet Propulsion Laboratory (Fig. 17), Chariot is under development at Johnson Space Center (Fig. 18), K-10 is under development by NASA Ames Research Center, and Scarab is under development by Carnegie Mellon University in conjunction with NASA Glenn Research Center.[7,8,9,10]

The LSMS exceeded performance goals despite high winds, rain and wind blown debris. Table 1 provides a synopsis of the results for the week. The first column lists objects that were loaded and unloaded from an elevated platform 2m in height, the second and third columns provides dimensions and weight and the fourth column provides the average time to load and unload the object. Typically 5 runs were made with each object at different times during the day resulting in varying lighting conditions. No auxiliary lights and only 2 fixed cameras were used. The primary camera is visible in Fig. 15 mounted under the forearm, and a second camera mounted to a tripod provided an orthogonal view.

Payload unload, including engaging the hook, maneuvering the payload and disengaging the payload occurred more rapidly than expected, typically requiring less than 5 minutes per payload in a tele-operated mode. Wind hampered operations by causing the lifting link to move, thus complicating hook engagement, but was not a major factor.

Figure 16. LSMS on Elevated Platform Preparing to Offload Large Airlock Mockup.

Table 1. LSMS Performance Data

Payload	Dimensions [in (cm)]	Weight [lbs (N) in 1 g]	Unload Time [min]
Airlock Mockup	90 Diameter x 115 H (229 dia x 292 H)	480 (2135.1)	4.5
ISRU A	36 L x 21 W x 55 H (91 L x 53 W x 138 H)	110 (489.3)	4.8
LSEP	40 L x 19 W x 56 H (102 L x 48 W x 142 H)	250 (1112.1)	4.8
ISRU B	50 L x 37 W x 29 H (127 L x 94 W x 74 H)	120 (544.8)	4.8
ISRU C	47 L x 44 W x 43 H (120 L x 112 W x 109 H)	150 (667.2)	4.8

The LSMS proved to be a versatile lifting device. Payloads may be lifted either at mid-span as shown in Fig. 16 or at the tip as shown in Fig. 15. Neither of these operations required a conventional hoist. Both used a lifting link deployed from the arm or forearm. This is a new approach to payload operations first demonstrated at Moses Lake made possible by the unique design of the LSMS. As shown in Figs. 16, 15 and 17, the LSMS is capable of operating either from the elevated platform, a ground mount or a mobile base.

The LSMS is a precision device enabling compact packaging of the launch vehicle. The ability of the LSMS to lift or grapple payloads from either the top or sides enables payloads to be packed without gaps, significantly improving packaging density both on the launch vehicle and the lunar mobility vehicle. Precision placement of a simulated ISRU unit on Chariot was accomplished at Moses Lake as shown in Fig. 18. As an experiment of opportunity (i.e. not preplanned) the objective was to investigate potential problems and design drivers for future experiments. Placement was straight forward with 2 modes evaluated. One where the LSMS performed the placement with the vehicle stationary, a second where the payload was held approximately 12 inches from the deck and chariot positioned itself under the payload prior to the final downward motion by the LSMS. Both modes were successful; the major finding of the experiment was that in a tele-operated mode, an indication of range is desirable to allow the LSMS operator to monitor distance to contract.

IV. Future Plans

There will be two major areas where LSMS development will focus in the future. First, development will focus on the operational versatility of the LSMS architecture. The forklift mode shown in Fig. 1 enables the LSMS to reach under platforms or shelters to manipulate payloads. To perform these operations end-effectors capable of grappling payloads from either the side or bottom will be used. These end-effectors are expected to plug into the tool interface at the tip. Secondly, the LSMS architecture supports self motion, enabling the LSMS to self unload

Figure 17. LSMS Mounted to ATHLETE performing offload of simulated ISRU from Elevated Platform.

Figure 18. LSMS Performing Precision Placement of Payload on Chariot.

from a lander, transition from one base location to another, etc. To demonstrate these capabilities, a method of automatically disengaging, engaging and leveling the base is needed. This will be a focus of the upcoming year.

V. Conclusions

The first generation test-bed of a new high performance device, the Lunar Surface Manipulation System (LSMS) has been designed and built. During laboratory tests, the LSMS closely matched structural analysis predictions. It successfully demonstrated operational capabilities during field tests at Moses Lake, Washington. In these field tests both large and small payloads were routinely removed from and loaded onto an elevated platform, typically in under 5 minutes per payload. Each sequence involved engaging a hook on the payload, lifting the payload and then positioning it either on the surface (unloading) or elevated platform (loading) then disengaging the hook in a tele-operated mode. The performance was more impressive due to the high wind loads at the field site, an environmental load not present on the moon. The LSMS has many unique features resulting in a mass efficient solution to payload handling on the lunar surface. Typically, the LSMS device mass is estimated at approximately 3% of the mass of the heaviest payload lifted at the tip, or 1.8 % of the mass of the heaviest mass lifted at the elbow or mid-span of the boom for a high performance variant incorporating advanced structural components. A unique feature in the design are spreaders that engage to act like spokes on a wheel to maintain mechanical advantage about the joints as the joint rotates. These same spreaders disengage allowing the tension members to lift off for improved joint range of motion providing a large operational workspace and enabling unique operational configurations such as a fork-lift mode to allow the LSMS to reach under landers or shelters as well as operational modes where the LSMS tip is positioned below its base to provide payload handling capabilities from Landers or into trenches. In addition, the LSMS can relocate its base enabling the LSMS to walk off the lander or move from a mobility vehicle to a fixed location. Also, the LSMS structural architecture places pure compression and tension on most primary structural members greatly simplifying transition to composite materials for mass savings. Finally, the LSMS is designed to package compactly for launch and then self deploy once on the lunar surface. The next major engineering challenge is to redesign the base to support automatic engagement and disengagement.

References

[1] Adinolfi, P.J.; Heinz, F.A. Jr: "Design Study of Special Purpose Systems For the Lunar Surface," NASA CR-61077, April 30, 1965.

[2] Eagle Engineering, "Lunar Surface Construction & Assembly Equipment Study: Lunar Base Systems Study Task 5.3," NASA-CR-172105, September, 1988.

[3] NASA, "NASA's Exploration Systems Architecture Study," Final Report, NASA-TM-2005-214062, 2005.

[4] Shapiro, H. I., et al, Cranes and Derricks, McGraw-Hill, Inc, 198**0**, 2n**d** ed. 1991.

[5] Dorsey, J.; Mikulas, M.; Doggett, W. Preliminary Structural Design Considerations and Mass Efficeincies for Lunar Surface Manipulator Concepts. Space 2008, Sept. San Diego CA.

[6] Dogget, W.; Dorsey, J.; Collins, T.; King, B.; and Mikulas, M.: A Versatile Lifting Device for Lunar Payload Handling, Inspection and Regolith Transport Operations. Proceedings of Space Technology and Applications International Forum – STAIF 2008. AIP Conference Proceedings Volume 969, Editor Mohamed S. El Genk, American Institute of Physics, 2008.

[7] Wilcox, B. H. ATHLETE: An Option for Mobile Lunar Landers. 2008 IEEE Aerospace Conference, Big Sky MT. pp. 1-8.

[8] Harrison, D.A.; Ambrose, R.; Bluethmann, B.; Junkin, L Next Generation Rover for Lunar Exploration. 2008 IEEE Aerospace Conference, Big Sky MT. pp. 1-14.

[9] Fong, T; Thorqe, C.; Baur, C. Multi-Robot Remote Driving With Collaborative Control. IEEE Transaction on Industrial Electronics, Vol. 50, No. 4 , Aug. 2003, pp. 699-704.

[10] Bartlett, P.; Wettergreen, D.; and W. L. Whittaker. Design of the Scarab Rover for Mobility and Drilling in the Lunar Cold Traps. International Symposium on Artificial Intelligence, Robotics and Automation in Space, Feb. 2008.